TUDelft

Delft University of Technology

A numerical assessment on the managed aquifer recharge to achieve sustainable groundwater development in Chaobai River area, Beijing, China

Liu, Sida; Zhou, Yangxiao; Luo, Weijia; Wang, Feiran; McClain, Michael E.; Wang, Xu sheng

Important note
To cite this publication, please use the final published version (if applicable).
Please check the document version above.

Research papers

A numerical assessment on the managed aquifer recharge to achieve sustainable groundwater development in Chaobai River area, Beijing, China

Sida Liu [a,b], Yangxiao Zhou [a,c,*], Weijia Luo [a], Feiran Wang [a], Michael E. McClain [a,b], Xu-sheng Wang [d]

[a] *IHE Delft Institute for Water Education, Westvest 7, 2611 AX Delft, the Netherlands*
[b] *Department of Water Management, Delft University of Technology, 2628 CN Delft, the Netherlands*
[c] *School of Water Resources and Environment, Hebei University of Geosciences, Shijiazhuang City 050030, China*
[d] *School of Water Resources and Environment, China University of Geosciences, Beijing 100083, China*

ARTICLE INFO

ABSTRACT

Intensive groundwater exploitation has depleted groundwater storage and led to a series of geo-environmental problems in Beijing Plain, China. Managed Aquifer Recharge (MAR) has been endorsed to mitigate the groundwater storage depletion and achieve groundwater sustainability. A pilot MAR has been tested in the Chaobai River catchment since 2015. An innovative large-scale MAR consisting of 9 cascade terraced infiltration ponds was proposed and its effectiveness was assessed in this study using an integrated modelling approach. The integrated model coupled the regional and local transient flow and transport processes. The transient regional flow model simulated historical groundwater level declines and storage depletion in the Beijing Plain from 1995 to 2018. The coupled regional and local flow model was used to simulate the pilot MAR test in the Chaobai River from 2015 to 2018. A significant groundwater level increase was observed nearby the pilot MAR since 2015. The transport model results indicate that approximately 40% of the infiltrated water was captured by pumping wells in the No.8 well field. The models were further used to assess the long-term effects of the large-scale MAR from 2020 to 2050. The simulation results show that the groundwater system will reach a new equilibrium state under the implementation of the large-scale MAR scheme. Almost 91% of the abstracted water in the No. 8 well field will come from the MAR infiltration. The proposed large-scale MAR is very effective in restoring the depleted aquifer storage and maintaining the groundwater abstraction in the No.8 well field. However, with the increase of the groundwater level, the infiltration rate of several ponds will decrease. Therefore, it is important to maintain a dynamic balance between artificial recharge and groundwater abstraction in order to achieve a sustainable long-term MAR operation in the region.

1. Introduction

Groundwater storage depletion has become a global issue that threats the sustainable water development (Aeschbach-Hertig and Gleeson, 2012; Famiglietti, 2014). Despite the impact of climate change, the long-term groundwater depletion is always resulted from intensive groundwater abstraction (UN-water, 2022). The Managed Aquifer Recharge (MAR) systems, which are widely applied globally, could help to enhance the groundwater recharge artificially and recover the aquifer storage (Bouwer, 2002; Dillon, 2005; Gale, 2005). The classification of MAR techniques has been summarized by IGRAC in the global MAR inventory report including the spreading methods, induced bank

filtration, well and borehole recharge that focus on getting water infiltrated; and in-channel modifications and runoff harvesting technique that focus primarily on capturing the water (IGRAC, 2007).

Among the techniques abovementioned, the spreading method in the river channel or by infiltration basin is a widely applied type of MAR globally, especially in the area with adequate land space and high permeable soil that allows water infiltration to the unconfined aquifer (Ghayoumian et al., 2005). The application of the spreading method usually combines with the source water capture system and recovery wells for water supply (IGRAC, 2007). The stormwater spreading system is implemented to augment the groundwater storage and decrease the peak discharge of the river as a flood control structure in the area with

uneven rainfall patterns (Hashemi et al., 2015; Yaraghi et al., 2019). In coastal area, reclaimed water is used to recharge the unconfined aquifer to prevent seawater intrusion (Abbo and Gev, 2008; Evans and Arunakumaren, 2012). Desalinated water has been used for injection without the concern of the clogging issue (Ganot et al., 2017). Lake or river water diverted from other regions can also be the source water for the water spreading for drinking water production (Mirlas et al., 2015; Olsthoorn and Mosch, 2002) or increasing the groundwater storage during the dry season (Barber et al., 2009) and reduce the groundwater depletion in the pumping intensive area (Izbicki et al., 2008; Pliakas et al., 2005; Teatini et al., 2015).

Numerical modelling as an effective tool for the design of the MAR system and the optimization of the MAR scheme, has been widely applied (Maliva et al., 2015). Groundwater flow model is the most frequently applied model type for the simulation of the MAR system (Ringleb et al., 2016). The main modelling objectives of the groundwater flow model include 1) identifying the suitable site for the MAR structures (Karimov et al., 2015; Rahman et al., 2013; Russo et al., 2015; Sashikkumar et al., 2017); 2) assessing the MAR performance (Barber et al., 2009; Neumann et al., 2004; Niswonger et al., 2017; Ronayne et al., 2017); 3) evaluating the impact of the MAR operation on the groundwater recharge dynamic (Masetti et al., 2016; Mirlas et al., 2015); 4) estimating the infiltration capacity (Ganot et al., 2017; Hsieh et al., 2010; Masetti et al., 2018; Namjou and Pattle, 2002); 5) optimizing the future MAR scheme (Lacher et al., 2014; Teatini et al., 2015; Xanke et al., 2016; Zeelie, 2002). Combined with the groundwater flow model, solute transport modelling is also applied frequently to 1) investigate the mixing process of the infiltrated water with the natural groundwater (Bahar et al., 2021; Vandenbohede et al., 2013); 2) examine the recovery efficiency of the MAR implementation (Huang and Chiu, 2018; Jarraya Horriche and Benabdallah, 2020); 3) assess the clogging issues by the geochemical processes (Soleimani et al., 2009).

To cope with the continuous groundwater storage depletion and the uncertainty of the future climate change in Beijing, utilizing MAR infrastructures to replenish the depleted aquifer has been considered in the last several decades (Zhang et al., 2008). Several potential artificial recharge sites has been selected (Yao, 2014; Zhang et al., 2013). The natural dry riverbed of the two main rivers in Beijing Plain have been recognized as ideal MAR sites for surface water infiltration and recharge of the shallow aquifer. Pilot MAR project has been implemented since 2015 (Cao et al., 2022; Zhou et al., 2021). Modelling studies have also been carried out to evaluate the performance of the current MAR implementation and the potential of the future MAR operation in Beijing (Hao et al., 2014; Hu et al., 2019; Ma et al., 2020; Nan et al., 2016; Xu et al., 2022; Zhou et al., 2012). However, most of these modelling studies were only dedicated to the local-scale simulation of MAR sites with relatively short simulation period, which lack the capability to evaluate the contribution of the MAR operation to restoring the groundwater depletion of the entire plain region and support the decision making for an integrated groundwater management of the city. In addition, the boundary conditions of local modelling studies are normally defined as no flow or constant head boundary based on the groundwater contour map. The uncertainty caused by the boundary conditions on the predicted result for the future scenarios has been addressed by different researchers (Liu et al., 2009; Rojas et al., 2010; Wu and Zeng, 2013).

This paper aims at assessing the effectiveness of achieving sustainable groundwater development in the Chaobai River area by implementing a large-scale MAR in the riverbed. An innovative MAR system consisting of 9 cascade terrace infiltration basins was designed in the 12 km long riverbed for artificial groundwater recharge. With the multiscale groundwater flow and solute transport models, the local MAR system in the Chaobai River and the regional groundwater flow in the Beijing Plain can be simulated simultaneously. Therefore, a unique modelling strategy was carried out in a number of steps. Firstly, a regional transient groundwater flow model was constructed from 1995

to 2018 to assess groundwater depletion in the Beijing Plain. Secondly, a local groundwater flow model was developed for the pilot MAR in the Chaobai River coupled with the regional flow model. The movement of the infiltrated water was tracked with a tracer transport model Thirdly, the long-term effect of the designed large-scale MAR was simulated with the coupled model from 2020 to 2050. The findings from the model simulations support the implementation of the large-scale MAR as an effective measure to achieve sustainable groundwater resources development in the area.

2. Materials and methods

2.1. A review of groundwater model development in Beijing Plain

The area of Beijing has the typical characteristic of a piedmont plain surrounded by mountains in the north and west (Zhou et al., 2013). The long-term average annual precipitation and open pan water evaporation are 593 mm and 1728 mm, respectively. The temporal distribution of the rainfall is very uneven throughout the year. 75 % of the total rainfall occurs during the raining period from June to September. Two large rivers, Chaobai and Yongding, run dry most time since reservoirs were constructed at upstream. In recent years, Beijing municipality started to rehabilitate these two rivers and implement pilot managed aquifer recharge. The aquifer system varies from an unconfined aquifer near the foot of the mountains to multi-layered semi-confined aquifers downstream of the plain. Groundwater provides almost two-thirds of the water supply for Beijing City. To manage the groundwater resources of the Beijing Plain, regional groundwater studies began in the 1990s. In 1995, an investigation of the groundwater resources in Beijing was carried out. Groundwater storage and water budget components were calculated and analysed, which provided solid information for the construction of a regional groundwater model of the Beijing Plain. A three-dimensional transient groundwater flow model was built to evaluate the groundwater resources from 1995 to 2005 using MODFLOW-2000 (Han, 2007). This transient flow model was extended to 2010 to analyse options for sustainable groundwater resources development (Zhou et al., 2012). Based on the previous modelling study, an alternative model was constructed with the so-called "true-layer" model approach (Fig. 1(a)) where model layers were truncated with the actual extension of aquifers and aquitards (Liu et al., 2021a). The conceptual model consists of five aquifers and four aquitards. Nine model layers were used to represent every aquifer and aquitard. This regional model was calibrated in the steady state using the recharge and discharge data of the year 1995, in which the total groundwater recharge and discharge are approximately balanced. Afterwards, coupled regional and local scale models with different refining methods were constructed and evaluated for the simulation of the MAR scheme in the Chaobai River catchment (Liu et al., 2021b).

2.2. Extension of the regional transient groundwater flow model

A new transient regional flow model was developed in this study to simulate groundwater flow changes in Beijing plain from the year 1995 to 2018 with a monthly stress period using the MODFLOW 2005 program in GMS modelling environment (Aquaveo, 2019). The total model area is 6,642 km^2 and was discretised with a uniform grid of 1000 m by 1000 m. The model consisted of 9 model layers corresponding to 5 aquifers and 4 aquitards. In total, 23,300 active cells were included in the model simulation. The transient inputs of the old transient model for 1995 to 2010 were adopted and the model was extended to 2018, including recent changes in the reduction of groundwater abstractions since the delivery of the new water source to Beijing from the South to North Water Diversion project by the end of 2014. The main sources and sinks of the flow model are depicted in Fig. 1(a). Monthly groundwater recharge series were extended using monthly meteorological data from 2011 to 2018 and simulated by the Recharge (RCH) package. Infiltration
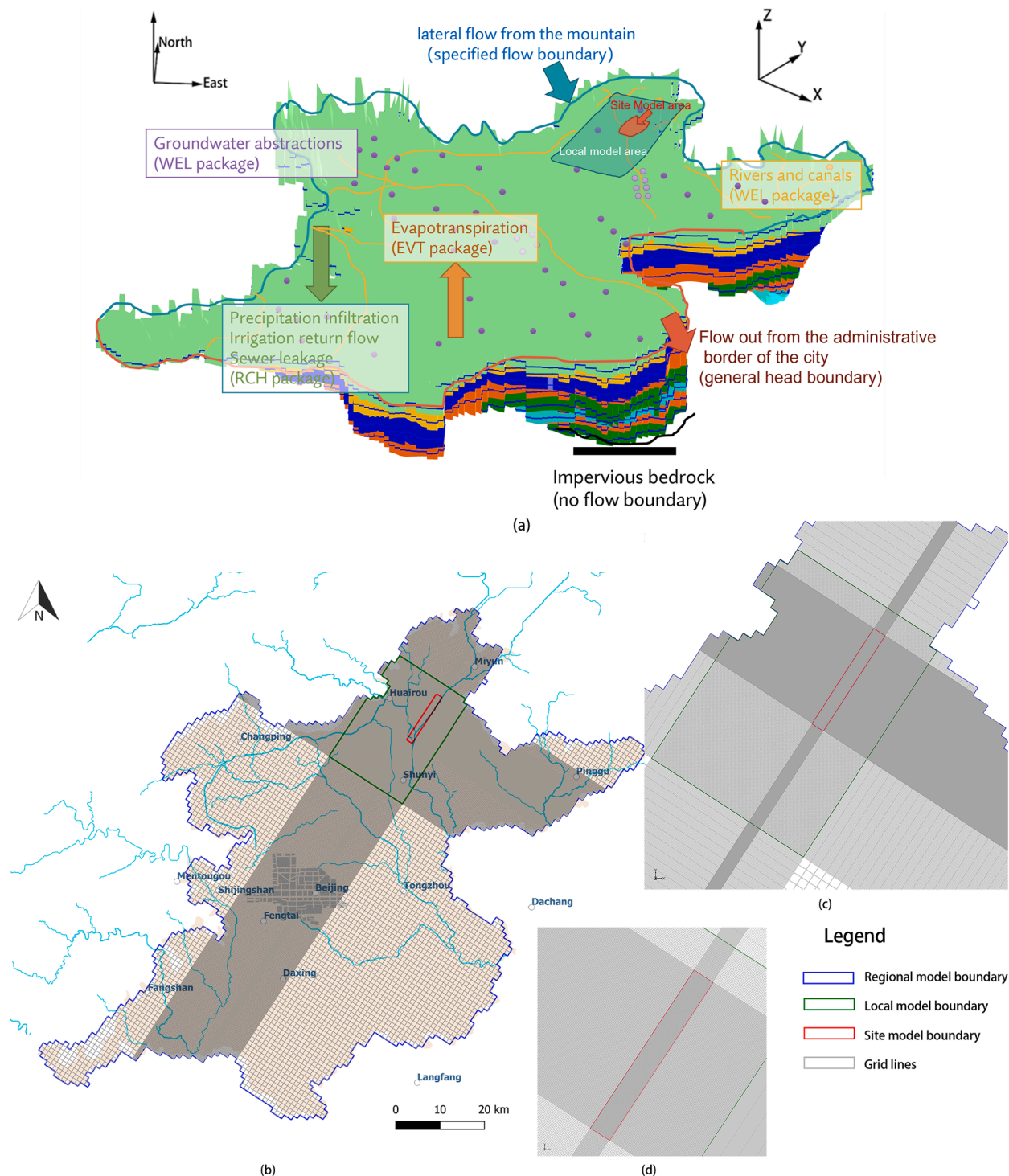
Fig. 1. (a) The conceptual model of the coupled regional and local groundwater flow model of the Beijing Plain (revised from Liu et al., 2021b)). Each colour represents one model layer. (b)-(d): Grid of the multi-scale models: (b) regional model (1000 m × 1000 m); (c) local model (100 m × 100 m); and (d) site model (20 m × 20 m). The blue, green and red lines are the boundaries of the regional, local and site models, respectively. (For interpretation of the references to colour in this figure legend, the reader is referred to the web version of this article.)

coefficients were assigned to recharge zones based on the characteristic of the land surface and soil type. Map of the infiltration coefficients can be found in Supplementary Materials A. Groundwater evaporation was simulated by the Evapotranspiration (EVT) package derived from the pan evaporation data. Abstraction was simulated by the Well (WEL) package and categorized into four types: industrial use, agricultural use, township water supply, and urban water supply well fields. The annual groundwater abstractions for different usages were obtained from the

Beijing Water Resource Bulletin (Beijing Water Authority, 2021). The total amount of abstraction was allocated to each district and mapped to the corresponding grid cells in the model. Irrigation return flow was calculated based on the annual agricultural groundwater use and simulated by RCH package. Pipeline leakage was simulated also by RCH package and specified as a constant value in the city centre area. Since the rivers are dry most time and have water only during raining periods. The amount of leakage was computed for raining periods and was

simulated as injection rates in WEL package. Lateral boundary flow from the mountainous region was derived from the annual water balance calculation of the Beijing Plain and simulated as injection wells by WEL package. The administrative borders in the south and east were specified as head-dependent boundary simulated by General Head Boundary (GHB) package. Afterwards, these model inputs were examined and adjusted by an inverse modelling process to check the consistency of the computed and observed groundwater level time series. The hydraulic conductivities were optimised with PEST in the previous model study (Liu et al., 2021b). The specific yield and specific storage values were obtained from the previous transient model (Zhou et al., 2012) and manually adjusted for better model fit. This calibrated model was used for the evaluation of the groundwater level and storage changes in response to the reductions of groundwater abstraction and to couple a local flow model for the design and simulation of the MAR scheme in the Chaobai River.

2.3. Simulation of pilot MAR in Chaobai River with multi-scale transient models

To simulate the MAR operation in the Chaobai River catchment, the regional model grid was refined with the conventional grid refining method with variable spacing and the grid lines in each direction extends out to the model boundary Chaobai River area into a local model grid and a site model grid in MODFLOW-2005 (Fig. 1(b)-(d)). The area of the local model is 561 km² and the uniform model grid size is 100 m. The area of the MAR site model is 26.6 km² with a uniform model grid of 20 m by 20 m. The determination of the local and site model boundary was tested iteratively which ensures the extents of the refined grid area are sufficient to capture the influence of the MAR operation on the local groundwater flow field.

The MAR site of the Chaobai River channel is dry most of the time throughout the year because the reservoir upstream captures most of the river discharge. The intense groundwater exploitation nearby the NO.8
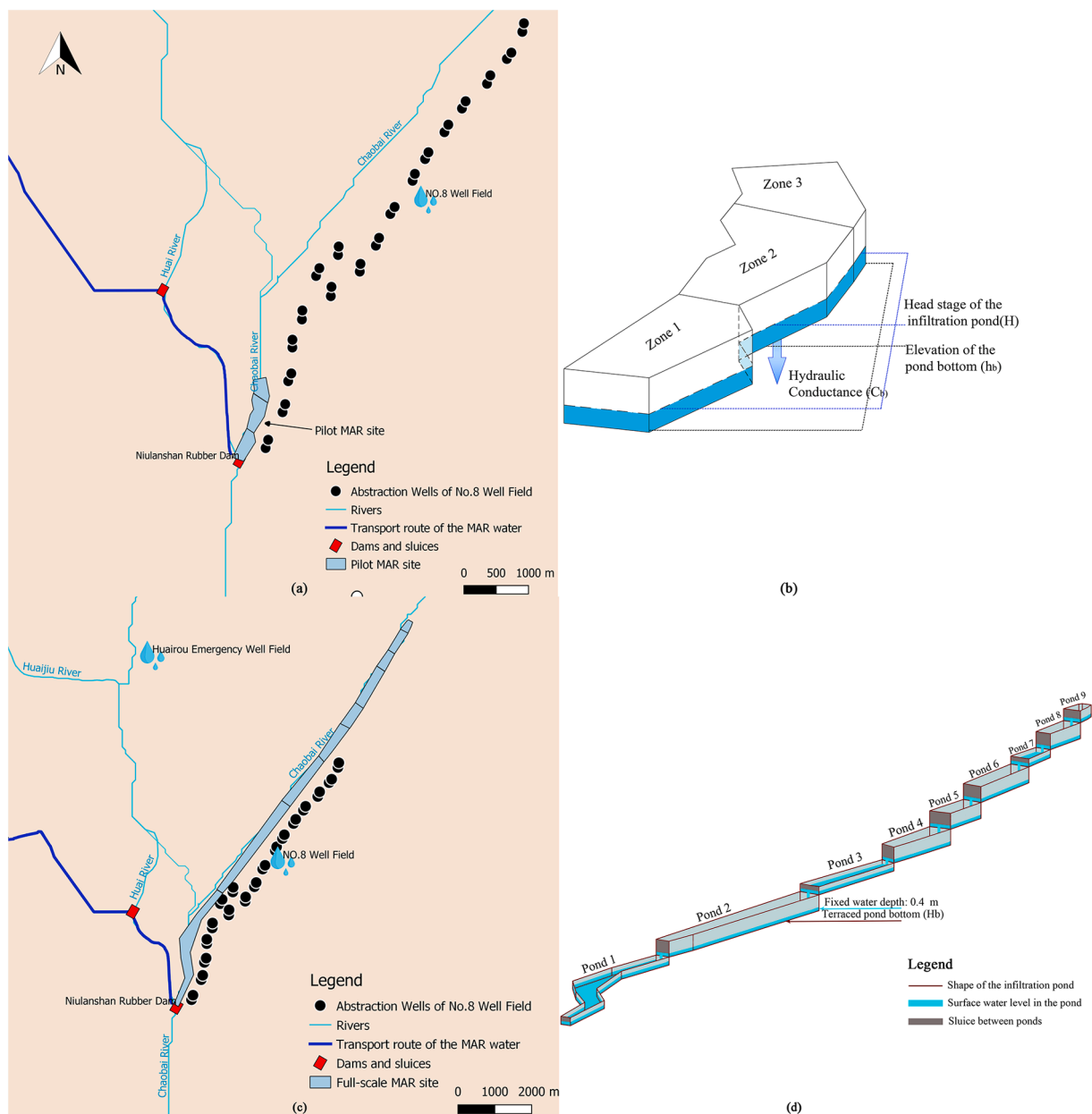

Fig. 2. Location of the Pilot MAR site (a) and the diagram of the MAR infiltration simulation in the MODFLOW RIV package (b). Location of the full-scale MAR site (c) and the layout of the full-scale MAR scheme consisting of nine cascade terraced ponds simulated with MODFLOW RIV package (d).

Well Field has created a large cone of depression in the surrounding area. A feasibility study showed that this section of the river channel is an ideal place for the implementation of the MAR system. The pilot MAR test started in 2015. Source water from the South to North Water diversion project (Webber et al., 2017) was transferred to the Niulan-shan Rubber dam and spread to the 1.5 km river channel (Fig. 2(a)). It has been verified that the quality of the source water reaches the standard of Category II based on the Chinese Standard of Groundwater Quality (AQSIQ and SAC, 2017), which is better than the natural groundwater quality. Thus, the risk of clogging problem caused by the artificial recharge is minimal.

The groundwater flow model was designed to simulate the variation of the groundwater level during and after the pilot MAR test. The infiltration process was simulated with the River (RIV) package of the MODFLOW program. The 1.5-km river channel was divided into three polygons in the conceptual model (Fig. 2(b)). The required input data include the head stage of the infiltration pond (H), the elevation of the pond bottom (H_b) and the conductance of the riverbed (C_b). The flow rate of the source water to the infiltration pond was obtained from Beijing Water Authority. The water depth of the infiltration pond was obtained from the inflow rate, water release duration and the pond area. The riverbed conductance was calibrated to match the infiltration rate of the pond equal to the measured rate. Detailed input data can be found in Supplementary Materials A. In 2015, 33.7 million m^3 of water were infiltrated from the Chaobai riverbed between August and November. In 2016, 10.3 million m^3 of water were infiltrated in 15 days from July 20th. In 2017 and 2018, pprox.. 44 million m^3 of source water were infiltrated between May and November. The groundwater levels in the monitoring wells nearby showed a significant increase in response to the pilot MAR test. During the non-recharge period, the groundwater levels decreased because of the continued abstraction in the NO.8 Well Field. The head stage of the RIV package was set as the sum of the pond bottom elevation with the pond water depth during the recharge period. During the non-recharge period, the head stage was assigned the same as the pond bottom elevation so that no infiltration takes place. The conductance value was estimated based on the empirical value of the riverbed materials and calibrated by matching the computed river leakage with the inflow to the MAR site.

2.4. Design and simulation of a full-scale MAR in Chaobai River

The pilot MAR test in the Chaobai River has shown the feasibility of the implementation of a full-scale MAR system. In this scheme, a total of 12.4 km dry riverbed was designed to be converted into nine terraced infiltration ponds with different lengths elevated from south to north (Zhou et al., 2021). As is shown in Fig. 2(c), the total recharge area is approximately 3.03 km^2. The layout of the full-scale MAR scheme is shown in Fig. 2(d). The source water is designed to flow into the MAR infiltration ponds from the inlet at the upstream infiltration pond (pond 9). The artificial recharge is planned from April to November each year with a 14 m^3/s inflow rate of the source water. The maintenance of the infiltration ponds will be done during the non-recharge period. In total, 1.121 million m^3 of water can be recharged daily to the unconfined aquifer beneath the MAR site. The estimated annual recharge capacity is about 290 million m^3.

For the simulation of this full-scale MAR operation, the terraced infiltration ponds were conceptualized into nine polygons. The bottom elevation of the pond and the conductance of the pond bottom were assigned to each polygon. The water depth in each pond was set as 0.4 m, which was derived from the designed inflow rate of the source water. The properties of these nine infiltration ponds are specified in Table 1. To simulate the long-term effect of the full-scale MAR operation, the simulation period was set from the year 2020 to 2050 with the monthly stress period. Other sources and sinks were kept the same as the current situation.

Table 1
The designed dimension of infiltration ponds for the long-term MAR operation.

Pond number	Width (m)	Length (m)	Pond bottom elevation (m)	Head stage of the infiltration pond during the recharge period (m)	Hydraulic conductance (m^2/d)
Pond 1	350	3400	31	31.4	360 for all ponds
Pond 2	250	2900	32	32.4	
Pond 3	270	1700	34	34.4	
Pond 4	260	1100	35	35.4	
Pond 5	250	690	37	37.4	
Pond 6	260	1200	39	39.4	
Pond 7	200	530	41	41.4	
Pond 8	215	620	42	42.4	
Pond 9	170	300	44	44.4	

2.5. Tracking the movement of infiltrated water with hypothetical tracer using transport model

The groundwater flow models of the MAR simulation can help to analyse and predict the recovery of the groundwater head and storage. The mixing process of the MAR infiltrated water with the native groundwater needs to be simulated by a solute transport model (Ganot et al., 2018; Lautz and Siegel, 2006; Ronayne et al., 2017). In this study, we are interested to track water particles from the infiltration pond to arrival at pumping wells in the No.8 Well Field. So, the hypothetical tracer representing water particles was simulated only with advective transport using M3TDMS (Zheng and Wang, 1999). Because of the stable and continuous groundwater abstraction of the NO.8 Well Field, the infiltrated MAR water will partially be captured by the abstraction wells used for the urban water supply and partially stored in the aquifer as storage. The groundwater abstracted from the No.8 Well Field (Q_{abs}) is the summation of the groundwater from two sources: a) natural groundwater ($Q_{natural}$) and b) MAR infiltration (Q_{MAR}). A hypothetical tracer was created to simulate the transport of the infiltrated water by the MT3DMS program. The tracer concentration in the MAR infiltration ponds (C_{MAR}) was set as 100 mg/L. Only advective transport with MOC method was considered in this case which means the tracer is conservative and only moves with groundwater flow. The concentration of the natural groundwater ($C_{natural}$) was defined as 0 mg/L. Thus, the concentration of the tracer at the No.8 Well Field (C_{abs}) can be computed by the solute transport model. The water balance and mass balance equations of the tracer can be written as follows:

$$Q_{natural} + Q_{MAR} = Q_{abs} \tag{1}$$

$$C_{natural} \times Q_{natural} + C_{MAR} \times Q_{MAR} = C_{abs} \times Q_{abs} \tag{2}$$

By dividing both equations with the well yield Q_{abs}, applying $C_{natural}$ = 0 mg/L and C_{MAR} = 100 mg/L into the equation (3). The fractions of the MAR infiltrated water to the well (f_{MAR}) can be derived as Eq. (4):

$$C_{natural} \times \frac{Q_{naturaal}}{Q_{abs}} + C_{MAR} \times \frac{Q_{MAR}}{Q_{abs}} = C_{abs} \tag{3}$$

$$f_{MAR} = \frac{Q_{MAR}}{Q_{abs}} = \frac{C_{abs} - C_{natural} \times \frac{Q_{natural}}{Q_{abs}}}{C_{MAR}} = \frac{C_{abs}}{100} \tag{4}$$

Thus, the tracer concentration at the well field is equivalent to a mixing percentage of the MAR water with the natural groundwater. With this solute transport model, the mixing process was traced, and the movement of the MAR water was tracked. In addition, the contribution of the MAR water to the groundwater abstraction at the No.8 Well Field was quantified by checking the mass balance of the solute transport simulation result.

3. Results

3.1. Transient model calibration

The transient regional groundwater flow model was calibrated by minimizing the residuals of the computed and observed groundwater head by trial and error. Detailed model calibration information can be found in Supplementary Material A. The time-series of the computed and observed groundwater head in three wells in three typical locations are plotted in Fig. 3. These fitting curves show that the computed heads mimic long-term variations of the observed heads. Groundwater levels in these 3 observation wells show a similar pattern of changes: a long-term trend of decrease and reversal of the decline in recent years. Observation well H01 is located in the shallow aquifer in the eastern plain area (Fig. 3(a)). The groundwater level in this well dropped about 7 m from 1995 to 2016. Seasonal periodic fluctuations indicate groundwater recharge in raining seasons. The groundwater level in observation well H02 located near the Beijing urban area shows a larger decrease of about 12 m until 2000. There are several drinking water plants surrounding the urban area mainly supplied by groundwater abstraction. The rapid decrease of groundwater levels occurred in observation well H03 located in the Chaobai River catchment. The groundwater level dropped more than 40 m from 1995 to 2014. This large decline in groundwater levels was caused by intensive groundwater abstraction by the No.8 Well Field and Huairou Emergency Well Field. The annual abstraction during the continuous drought from 1999 to 2010 was more than 200 million m^3 in the No.8 Well Field. To cope with the groundwater shortage, Huairou Emergency Well Field was installed in 2003, which provided over 240 million m^3 of water every year during the drought period. In this period, an estimated 1.28 billion m^3 per year of groundwater was abstracted by these two well fields. The arrival of the "south water" from the South to North Water Diversion Project by the end of 2014 has reversed the trend of decrease. Since 2015, the Huairou Emergency Well Field has stopped operation, and the

annual groundwater abstraction in the No.8 Well Field has been reduced to approximately 60 % compared to the drought period. Combined with the artificial groundwater recharge in the Chaobai river channel, the groundwater level has recovered in recent years.

3.2. The overexploitation of groundwater resources in Beijing Plain

In general, due to the frequent drought and intensive groundwater abstraction, the groundwater level has decreased from 1995 until 2015 in most of the area. Fig. 4(a)-(c) shows the simulated groundwater head distribution in the shallow aquifer. A cone of depression gradually developed at the No.8 Well Field near the proposed MAR site in the last 20 years. The maximum drawdown reached 50 m near the No.8 Well Field in 2014. After the pilot MAR operation at the Chaobai MAR site, the cone of depression was reduced in 2018.

The simulated groundwater head distribution in a deeper aquifer (the third aquifer from the top) is shown in Fig. 4(d)-(f). the cone of depression in the deep confined aquifer was caused by the over-exploitation for industrial water supply. Since the leakage of groundwater in the shallow aquifer to the confined aquifer takes time, groundwater levels in the confined aquifer are still decreasing. The short-term MAR operation has not yet contributed to restoring the storage depletion in deeper aquifers. It will take a longer operation time before the MAR water reaches deeper aquifers.

Fig. 5 shows changes of major groundwater balance components and the cumulative groundwater storage change of the Beijing Plain. The majority of groundwater recharge comes from precipitation infiltration and inflow from mountainous areas which varies depending on rainfall amounts. Groundwater abstraction dominates groundwater discharge. Two major events had marked impacts on groundwater resources in the Beijing Plain. The consecutive drought from 1999 to 2010 reduced natural groundwater recharge and emergency groundwater abstraction to cope with the drought increased total groundwater abstraction. These combined effects accelerated groundwater storage depletion since 1999
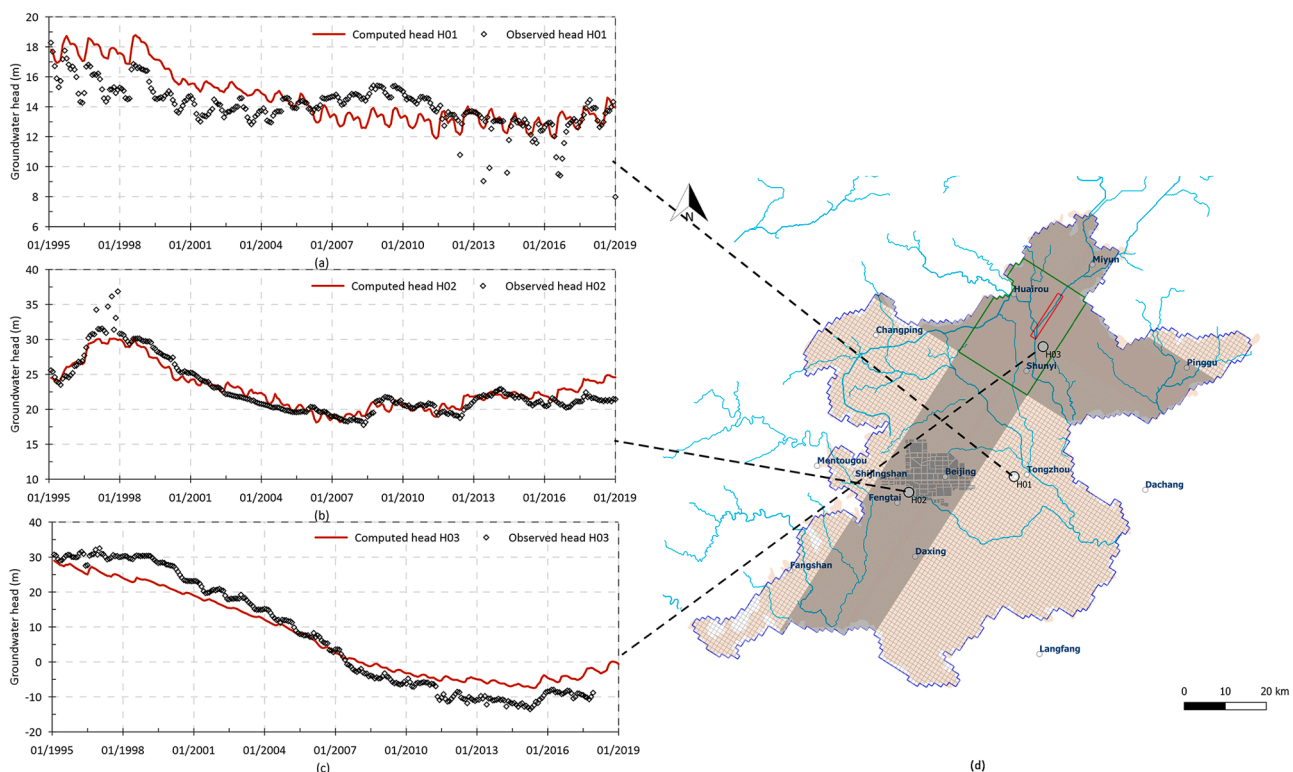

Fig. 3. Computed and observed groundwater head time series in Tongzhou District (a), Beijing urban area (b), and Chaobai River catchment (c). (d) Shows the locations of the three wells.
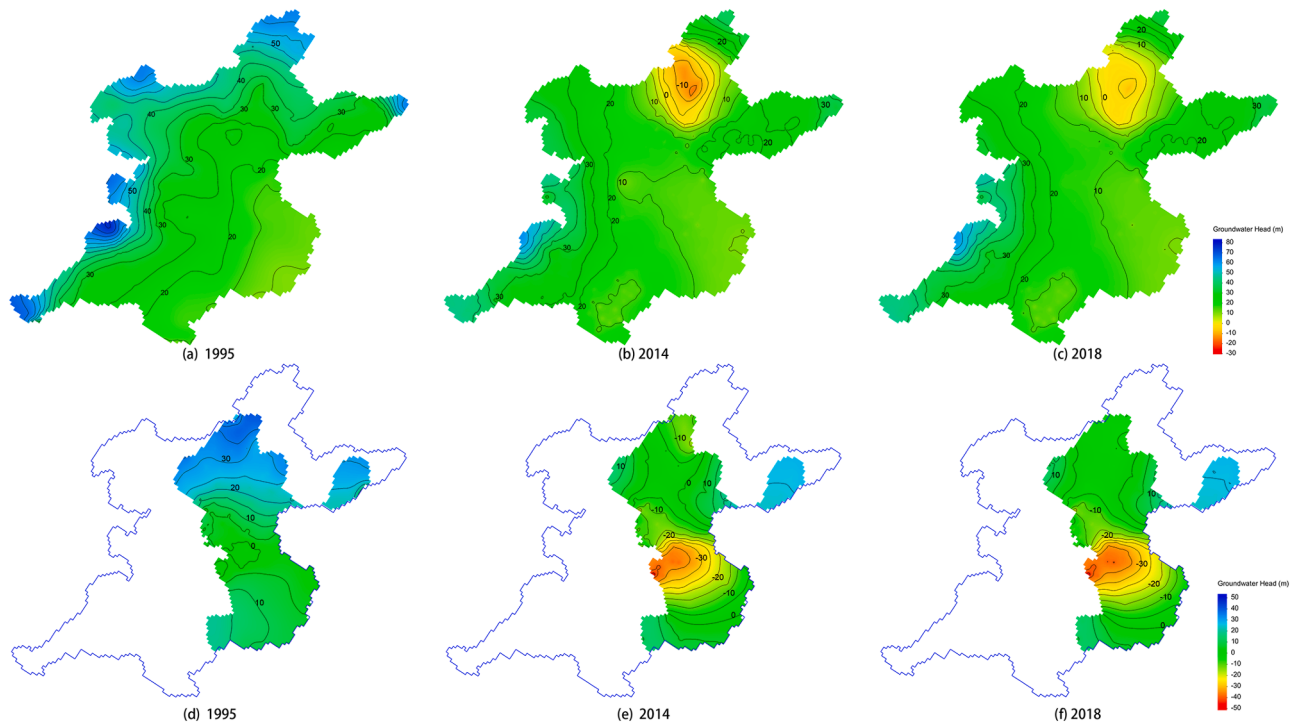
Fig. 4. Development of cones of depression in the shallow aquifer in January of (a) 1995, (b) 2014, (c) 2018 and in the deeper confined aquifer in January of (d) 1995, (e) 2014, (f) 2018.
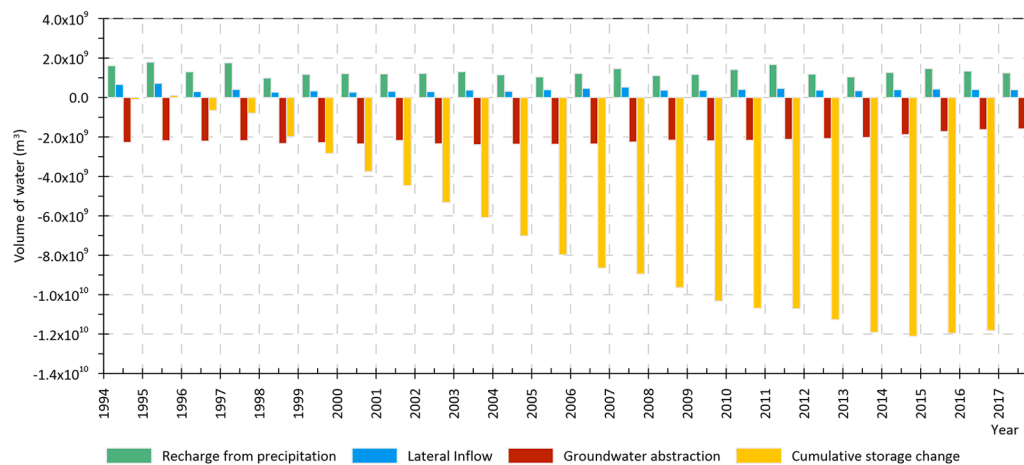

Fig. 5. Changes of major groundwater balance components computed from the regional groundwater flow model.

shown in Fig. 5. The cumulative storage depletion reached 12 billion m³ in 2014. The arrival of south water to Beijing stopped further depletion of groundwater storage with the reduction of groundwater abstraction since 2015. However, without increasing groundwater recharge to replenish the aquifer, it would be difficult to recover the depleted groundwater storage in Beijing Plain. Water balance for all flow components is listed in supplementary.

3.3. Effects of the pilot MAR operation in Chaobai River

The pilot MAR operation was simulated by the local and site groundwater flow model from 2015-2018. Fig. 6(a)-(c) show the computed and observed groundwater head of three observation wells near the Chaobai MAR site. The locations of these three wells are shown in Fig. 6(d). The computed heads show good consistency with the observed groundwater heads. The average residuals of the computed

and observed values of these three wells are −1.1 m, −0.36 m and −1.01 m. The groundwater head recovery process after the MAR implementation has been well captured by the local groundwater flow model. The groundwater level in the shallow aquifer responded quickly to the pilot MAR recharge. During the artificial recharge period, the groundwater level rises up significantly in the observation wells in the vicinity. After the end of each recharge period, the groundwater head was lowered due to the groundwater abstraction at the No.8 Well Field, but shows an increasing trend in general.

The decrease in the groundwater level in the Chaobai River catchment has been reversed and the groundwater storage has recovered since 2015. Both the reduction of the groundwater abstraction and the pilot MAR operation had contributions to the groundwater level increase in the Chaobai River area. The most significant increase in the groundwater level occurred near the Huairou Emergency Well Field. The head increase surrounding the MAR site has reached 10 m in these three
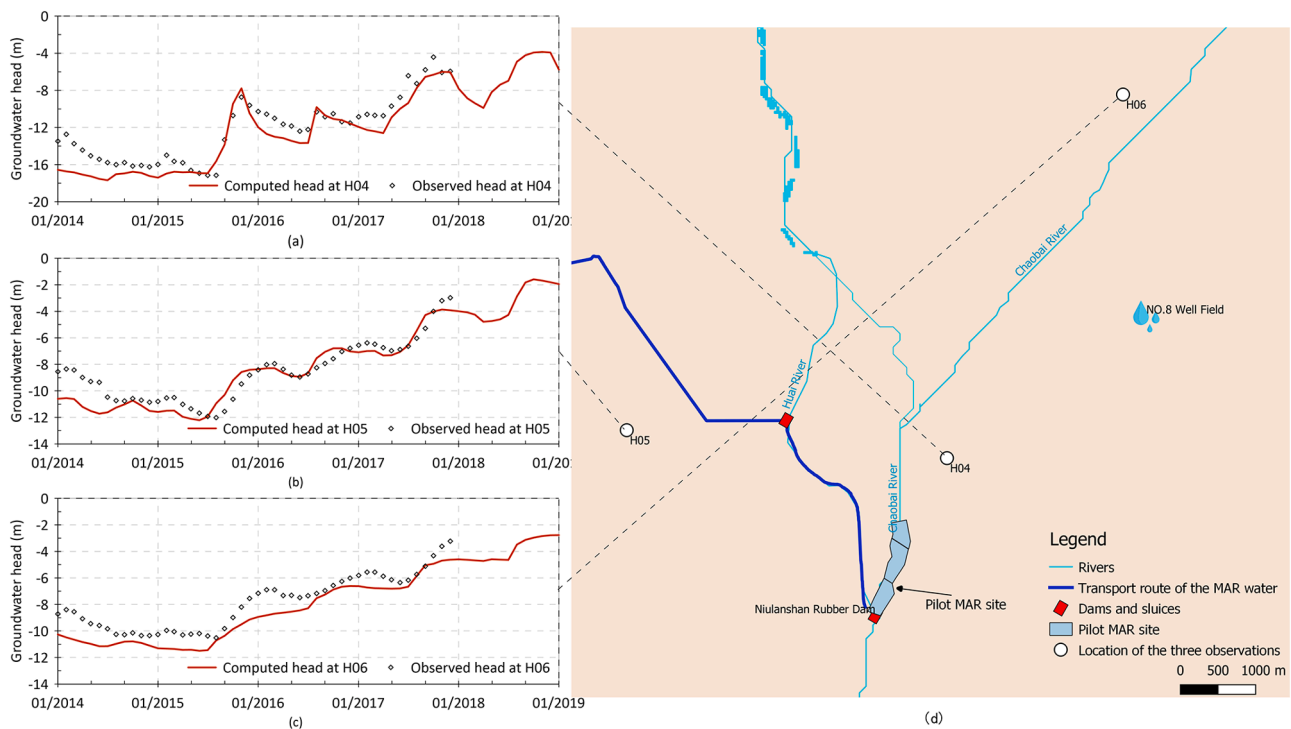
Fig. 6. The computed and observed groundwater level series near the MAR site. (a)-(c) show the computed and observed heads at three observation wells near the MAR site. (d) Shows the locations of the observation wells.

years. The groundwater head near the MAR site increased significantly and formed a groundwater mound near the area under the infiltration pond.

The subregional water budget of the Chaobai River catchment was computed with the Zonebudget program (ZONBUD) ([Harbaugh, 1990](#)) to analyse the monthly storage change ([Fig. 7](#)(a)) and cumulative storage change ([Fig. 7](#)(b)). Because of the intensive groundwater exploitation in the Chaobai River catchment, the groundwater storage was
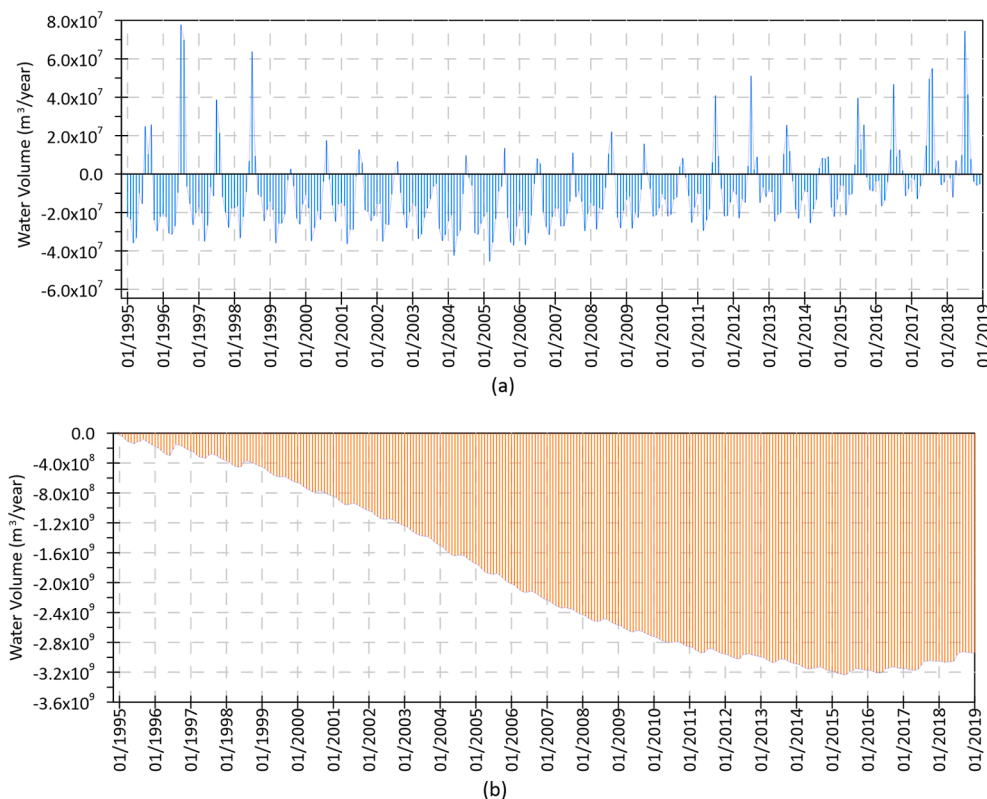

Fig. 7. Groundwater storage change in Chaobai River Catchment. (a) Monthly groundwater storage change (b) Cumulative groundwater storage change over 1995–2018.

depleted most of the time. The aquifer was only replenished during the rainy season. During the drought from 1999 to 2010, the aquifer storage barely recovered during the wet season. The cumulative groundwater storage depletion in the Chaobai River catchment reached more than 3 billion m^3 (Fig. 7(b)). After 2015, the aquifer received more artificial recharge with the MAR infiltration. The total recharge exceeded the total discharge, so that the groundwater storage depletion was reversed in the Chaobai River catchment.

3.4. Effectiveness of the full-scale MAR operation in the Chaobai River

The simulation of the full-scale MAR operation in the Chaobai River shows that with the nine terraced infiltration ponds, the groundwater level in the Chaobai River catchment can be notably recovered. Fig. 8 shows the predicted groundwater level change at the same 3 observation wells (well locations shown in Fig. 6(d)) near the MAR site and the predicted groundwater level distribution in the Chaobai River Catchment by the year 2050. After a 15-year operation of the full-scale MAR, the groundwater system will approach a new equilibrium state and the groundwater level will be nearly stable over the year. The minor variations in each year are caused by the seasonal change of the recharge and the suspension of the MAR operation during the winter months. Generally, the groundwater level would increase by 10 m to 20 m near the MAR site, which is very close to the ground surface. With this magnitude of groundwater level increase, the depleted aquifer will be replenished and the surface water in the infiltration ponds will have direct hydraulic connection with the groundwater. Fig. 8(d) is the predicted contour map of the Beijing Plain in the year 2050. Compared with the current situation, the large cone of depression in Chaobai River catchment will be recovered. The groundwater flow direction in the

north part of the plain will return to the natural condition of an alluvial fan.

The predicted storage change of the Chaobai River catchment is shown in Fig. 9. In the first seven-year operation, a high MAR infiltration rate and large groundwater storage recovery can be obtained. The total MAR infiltration can reach up to 270 million m^3 per year while the groundwater abstraction in the No.8 Well Field remains at approximately 127 million m^3 per year. The average annual storage recovery in the first seven-year operation will be about 180 million m^3/year. With an increase in groundwater storage in the area, the groundwater depletion will be reversed, and the cone of depression will be recovered. With this large-scale artificial groundwater recharge, the groundwater discharge to the downstream will increase to 40 million m^3/year in 2027. However, the storage recovery will slow down sharply afterwards because the MAR infiltration rate decreases with the increase of groundwater levels after 2027. By the year 2040, the annual MAR infiltration rate will be maintained at around 140 million m^3/year, and the discharge to the downstream area will be around 27 million m^3 every year. The system will reach a new equilibrium state in 2050 with the planned full-scale MAR operation.

4. Discussion

Numerical modelling of the groundwater availability is a useful tool for the groundwater management. It has been proved that fragmented and piecemeal arrangements are inadequate to meet the water challenge under the future change in climate and the human activities (Sophocleous, 2010). An integrated groundwater model that is continually updated and refined with new data and new groundwater-related projects are very important for the decision maker to evaluate the proposed
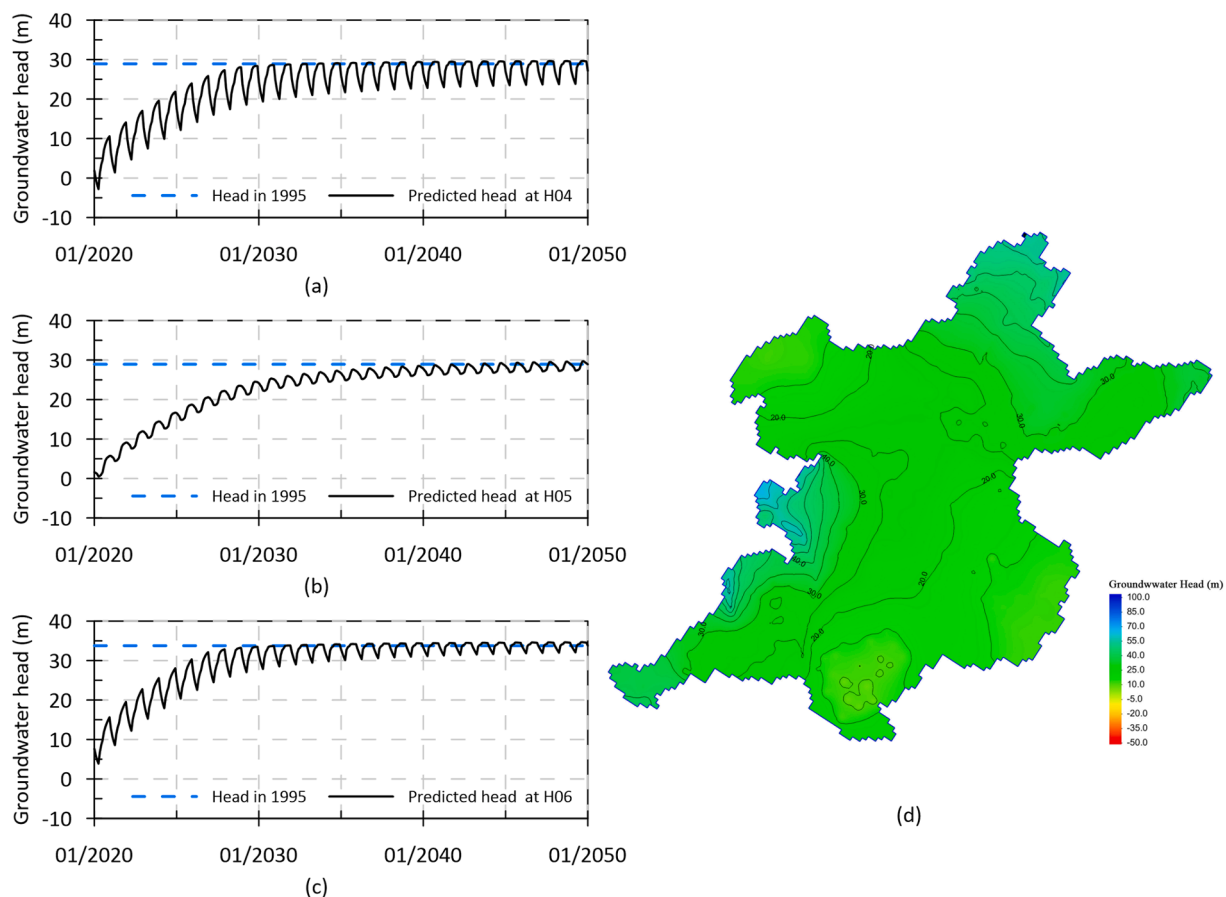

Fig. 8. Predictions of the groundwater head change in the three observation wells near the MAR site in the year 2020–2050 and the computed groundwater contour map of the Beijing Plain in 2050.
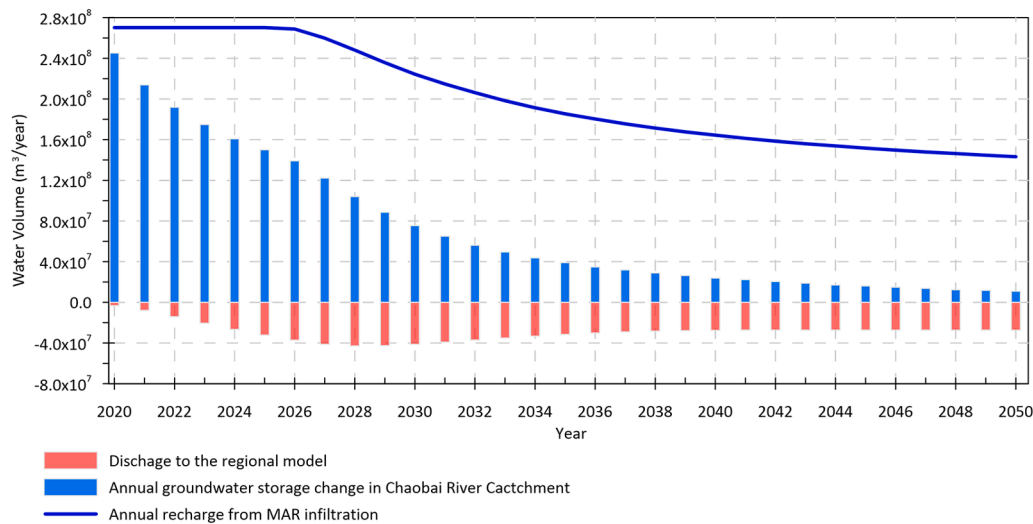
Fig. 9. Predictions of the annual aquifer storage change and recharge from the MAR infiltration.

groundwater management strategies, and formulate future policy towards the sustainable groundwater development (Gleeson et al., 2010; Sophocleous, 2010). In Beijing, modelling studies about the MAR implementation are mostly constructed on local scale for the demand of each specific project. For example, the groundwater modelling study for MAR in the Yongding River catchment included a model area of 888 km^2 and defined the western boundary as no flow boundary and the eastern boundary as the general head boundary (Ji et al., 2021). Flow and transport models were constructed in downstream Chaobai river in a 255 km^2 area to evaluate the impact of infiltrating reclaimed water into the riverbed. Constant head and general head boundary were applied (Jiang et al., 2022). These assumptions on boundary conditions may be adequate for the short-term simulation. However, groundwater flow dynamics could change dramatically in the region that is highly urbanised and with intensive human activities like Beijing Plain. The assumptions on the boundary conditions on the local model would lead to inaccurate long-term prediction results.

The multi-scale groundwater flow model in Beijing Plain we present in this study can overcome the deficiencies of previous model studies. The simulation of the local-scale MAR project will not be restricted by the boundary of the local model but interlinked with the regional groundwater flow model. Moreover, combining with the solute transport model, more insight can be obtained. However, the accuracy of the tracer transport simulation can be improved with a finer grid. We compared the simulation result from a finer grid model with a coarser grid model. It turns out that increasing grid resolution can delineate tracer distribution more accurately. Thus, a multi-scale model is an optimal choice to balance the computational time and the required accuracy of the solute transport simulation. More detailed discussion can be found in Supplementary Materials C.

4.1. The mixing of the infiltrated water with the native groundwater during the pilot MAR test

Fig. 10 shows the development of the mixing zone of the MAR water in different years represented by the concentration distribution. At the beginning of the MAR operation in 2015, the infiltrated water started to enter the aquifer shortly but only stayed beneath the infiltration ponds. With the formation of groundwater mound under the infiltration ponds, the infiltrated water was transported into the aquifer in all directions. A large portion of the MAR recharged water was captured by groundwater abstraction at the No.8 Well Field, which prevented the MAR water to move further to the east of the MAR site. After the 3-year artificial recharge, the mixing zone of MAR water reached 3.2 km^2 with 500 m to

700 m extent to each direction of the MAR site.

The contributions of the MAR infiltrated water to some abstraction wells are presented as breakthrough curves in Fig. 11. The arrival time and fraction of MAR water in the well depend on the location and distance of wells from the MAR site. The abstracted groundwater in Well 01 is 100 % MAR infiltrated water all the time since the beginning of the MAR operation. In Well 03 and Well 05, MAR water has become the dominant source during the recharge period. During the period without the artificial recharge, the proportion of the MAR water to the wells was reduced. In Well 07, only until the third year of the artificial recharge, a high percentage of MAR water was detected. The MAR water was not detected in other wells located the north of the infiltration pond further than Well 07.

The mass balance of the solute transport model has also been analysed. The total cumulative mass entering the aquifer from the infiltration ponds and total mass captured by the abstraction wells are plotted in Fig. 12. The ratio between these two mass volumes indicates the percentage of the MAR water abstracted by the No.8 Well Field. The graph shows at the beginning of the artificial recharge, the contribution of MAR water in the total abstraction is very limited. After three years, in total approximately 40 % of the infiltrated MAR water was abstracted by the No.8 Well Field and directly served for the domestic water supply of Beijing City. The other 60 % of the infiltrated water stayed in the aquifer contributing to the groundwater level recovery and storage restoration.

4.2. The long-term effect of the full-scale MAR operation on the Chaobai River catchment

The mixing process of the full-scale MAR operation has also been analysed to predict the future trend (Fig. 13). Generally, with the designed MAR scheme, the mixing zone of the MAR water and the native groundwater will keep increasing in the next 30 years. The area of the mixing zone will be developed from 27.64 km^2 in 2025 to 57.03 km^2 in 2035. However, after 2035, the development of the mixing zone becomes slower. The area of the mixing zone will be 61.86 km^2, 63.96 km^2 and 65.12 km^2 in the years 2040, 2045, and 2050, respectively. The shape of the mixing zone develops evenly in the west, north and south of the MAR site. The mixing zone has a limited extent in the east due to the continuous abstraction by the No.8 Well Field. The mixing zone can serve as the protection zone of the MAR site, which is also one of the key elements of the MAR project design. With the full-scale MAR operation, shallow groundwater levels will occur in the vicinity of the MAR site, which might cause the hazard of groundwater contamination and threatens the safety of the urban water supply. Thus, the solid waste
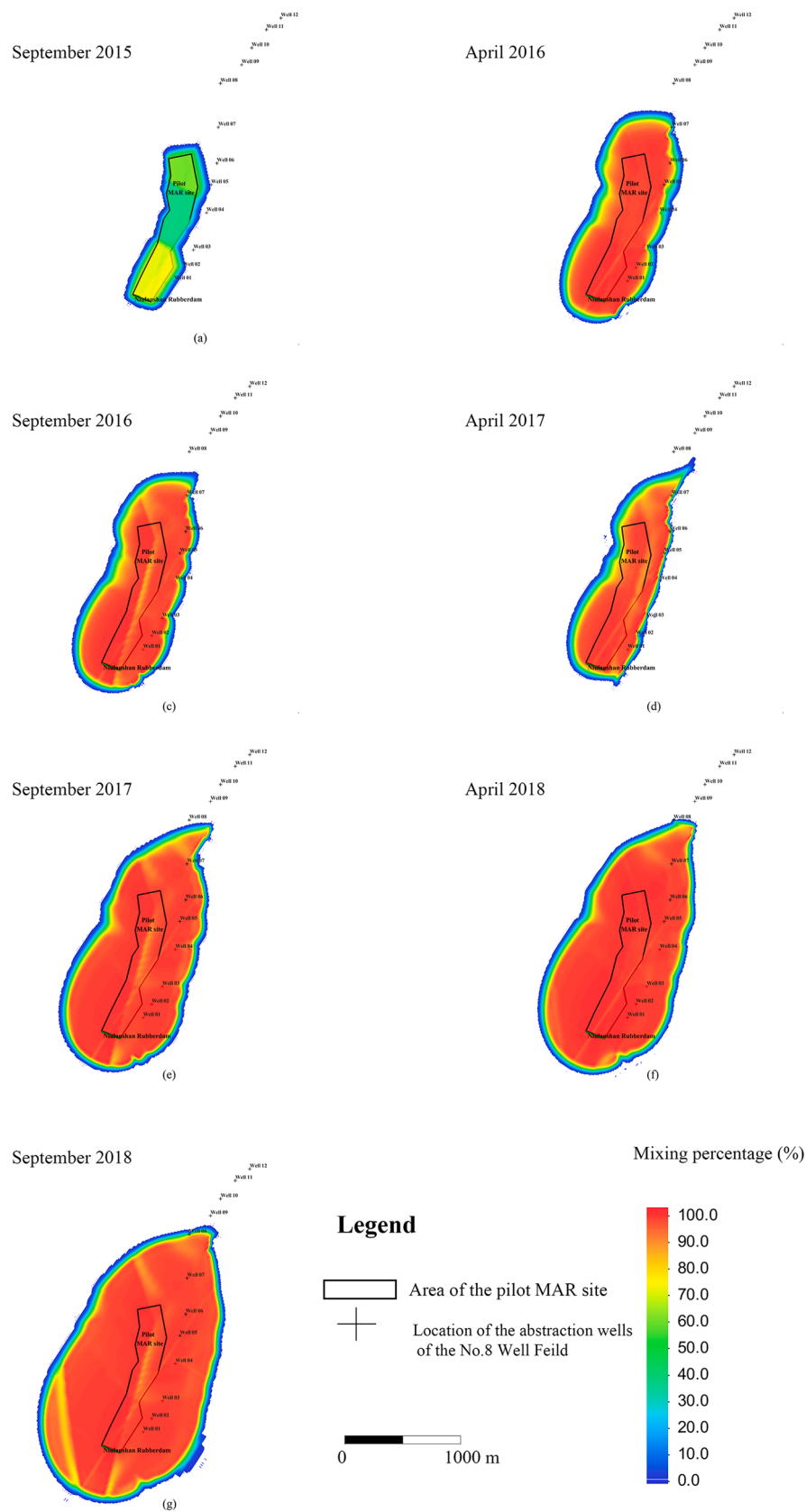
Fig. 10. Spreading of infiltrated water and mixing percentage of the MAR water with the native groundwater near the MAR site in the shallow aquifer.
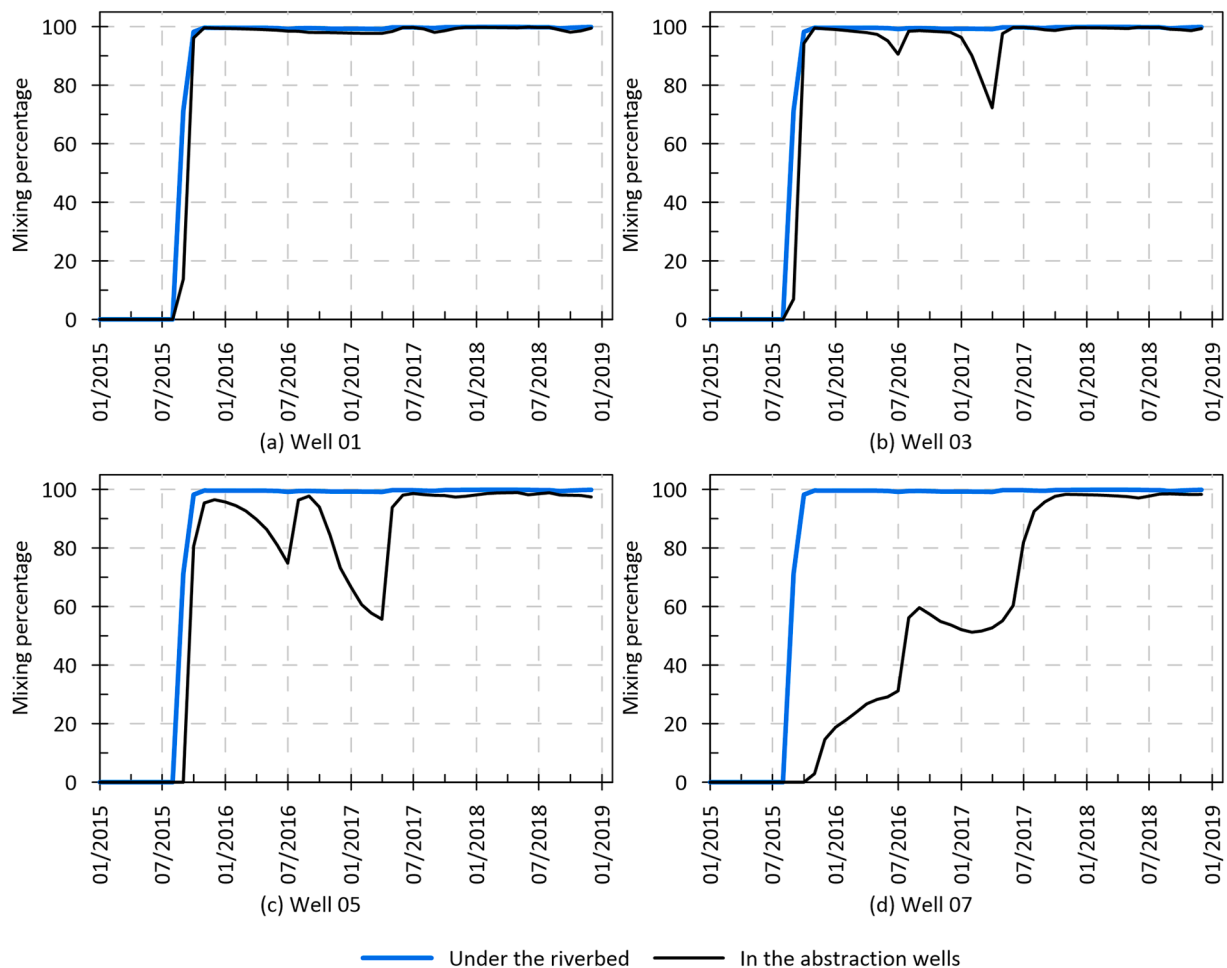
Fig. 11. The percentage of MAR infiltrated water to each abstraction well at No.8 Well Field.
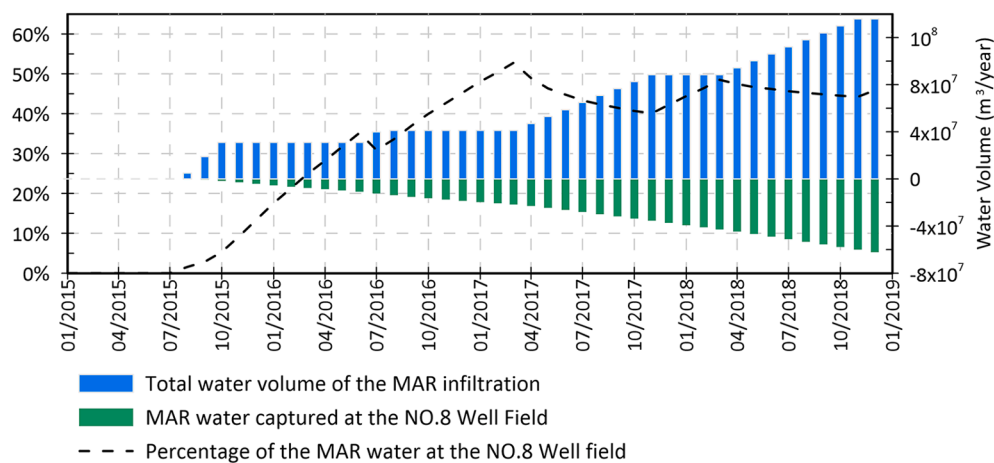

Fig. 12. The contribution of the MAR infiltrated water to the abstraction of the NO.8 Well Field during the pilot MAR project.

disposal sites in the mixing zone should be surveyed and evaluated before the full-scale implementation to avoid the risk of pollution.

The mass balance from the MT3DMS model (Fig. 14(a)) shows that at the beginning of the full-scale MAR operation, only 14.3 % of the infiltrated MAR water was captured by the pumping wells in the No.8 Well Field. With the spreading of the MAR water in the aquifer, more MAR water will be intercepted by the No.8 Well Field. Based on the cumulative mass balance result, by the year 2050, 58 % of the infiltrated

water will be abstracted for the urban water supply. 42 % of the infiltrated water will stay in the aquifer formed as groundwater storage. In this 30-year operation of the system, among the 6.2 billion m³ of water being infiltrated into the aquifer, 3.6 billion m³ will be abstracted for the urban water supply, which accounts for 91 % of the total groundwater abstraction at the No.8 Well Field. Thus, the water from the MAR project will be the major source for groundwater abstraction in the No.8 Well Field.
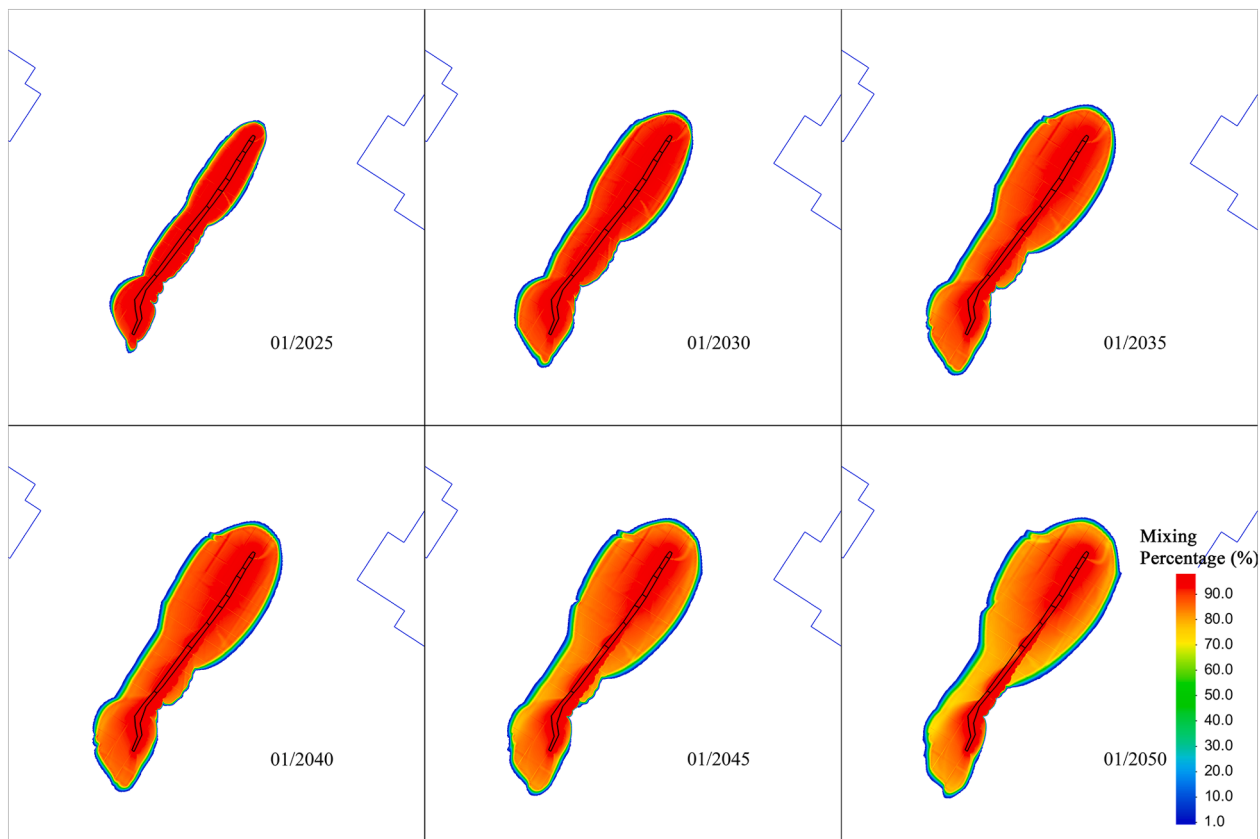
Fig. 13. Spreading of infiltrated water and the mixing percentage of MAR water with native groundwater after the long-term full-scale MAR operation in 2025–2050.

The predicted total groundwater budget of the Chaobai River catchment is summarised in Fig. 14(b). In the early stages, due to the high infiltration from the MAR implementation, the total groundwater inflow in the Chaobai area will be up to 530 million m^3 in 2020 and gradually lower to 350 million m^3 in 2035. With the groundwater level increase in the vicinity, the total outflow of the area will only slightly increase from 285 million m^3 to 333 million m^3 due to the larger discharge to the downstream aquifer. Thus, with the current groundwater management strategy, the groundwater storage will be accumulated rapidly at first and gently level off until asymptotic to the new equilibrium stage. The groundwater depletion caused by the over-exploitation from the last decades will be gradually compensated. Up to 2050, the cumulative storage increase in the Chaobai area will reach 2.2 billion m^3. It is convinced that the sustainable groundwater development of the Chaobai River region is achievable with the combination of the MAR implementation and groundwater management plan. However, the impact of the future climate change on the groundwater sustainability of the region still needs to be considered.

4.3. The decrease of infiltration rate of long-term operation of the full-scale MAR scheme.

In the current situation, the groundwater level is approximately 30 m lower than the bottom elevation of the infiltration ponds and the surface water is hydraulically disconnected with the groundwater. The aquifer will be recharged with the maximum infiltration rate. However, with the increase of the groundwater level above the infiltration pond bottom, the groundwater and surface water will be hydraulically connected, and the infiltration rate will gradually decrease. By running the long-term full-scale MAR simulation, the infiltration rate of each pond can be predicted. Fig. 15 shows the change in the infiltration rate with time for each infiltration pond. At the early stage of the full-scale MAR operation, all infiltration ponds can be operated with the maximum infiltration rate

because the groundwater levels are below the bottom of the ponds. However, with the current groundwater abstraction rate and the designed MAR recharge plan, the decrease of the infiltration rate will start in 2027 when the groundwater level in the south becomes higher than the bottom elevation of the infiltration ponds. Ponds 7, 8 and 9 in the north part of the MAR site will maintain a high infiltration rate because groundwater levels remain below the pond bottom in those areas. Among the nine infiltration ponds, the largest decrease in the infiltration rate occurs in the fourth pond, which is the pond where the predicted groundwater head reaches the pond bottom earliest. The infiltration rate of other ponds in the south (ponds 1, 2 and 3) will also drop to some extent. However, because of the existence of the No.8 Well Field, the infiltrated water will be abstracted for urban water supply. This groundwater abstraction forces extra infiltration capacity for ponds 1, 2 and 3 so that the long-term infiltration rate of these ponds can be still maintained between 0.2 m/d to 0.3 m/d by the year 2050. These results show that in the early stage of the MAR operation, the most important factor to obtain high infiltration capacity is the volume of the underground space. However, to design a sustainable long-term MAR scheme, it is vital to optimize the infiltration rate to ensure the infiltrated water can spread to the aquifer to a large extent as groundwater storage or can be directly abstracted for water supply. In the recent decade, reducing groundwater abstraction in the No.8 Well Field has been advocated and implemented. However, the reduction of the groundwater abstraction will also limit the infiltration capacity of the MAR system. For a mega-city like Beijing, increasing water demand is inevitable in the future. The implementation of the MAR and the groundwater exploitation are complementary. On the one hand, the MAR provides a secure water source for the groundwater abstraction. On the other hand, a moderate level of groundwater exploitation in the area can stimulate the potential of the MAR infiltration capacity.
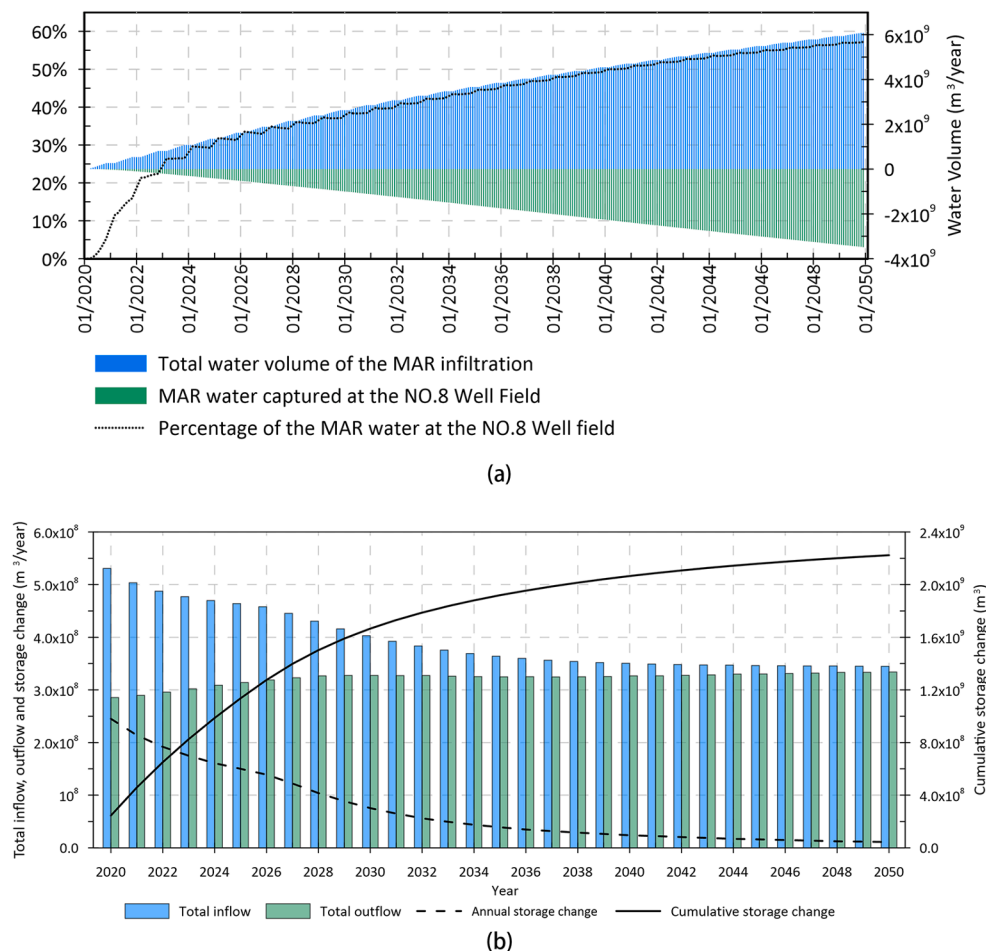
(a)

(b)

Fig. 14. (a) The predicted mixing percentage of the MAR infiltrated water abstracted from the No.8 Well Field under the full-scale MAR scheme. (b) The predicted annual total inflow, outflow, storage change and cumulative change of storage in the Chaobai River catchment from 2020 to 2050.
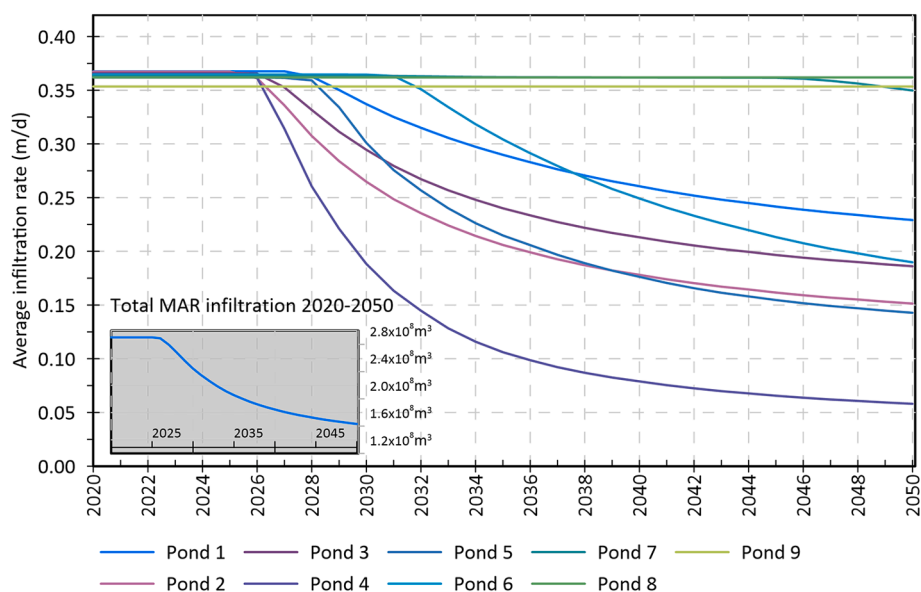

Fig. 15. Infiltration rate of each infiltration pond from 2020 to 2050.

5. Conclusions

The transient simulation of the regional groundwater flow from 1995 to 2018 revealed large changes in groundwater level and storage in the Beijing Plain. The severe groundwater depletion was exacerbated by the consecutive drought from 1999 to 2010 during which natural

groundwater recharge was reduced while groundwater abstraction was intensified. The South to North Water Diversion project was implemented and the south water from the Yangtze River arrived in Beijing in 2014 to substitute equivalent groundwater abstractions. Since 2015, the trend of groundwater level decline was reduced in the shallow aquifer.

The excess of the south water was also used for artificial groundwater recharge in the Chaobai River channel starting in 2015. The coupled multi-scale model simulation shows that the pilot MAR system has recharged approximately 130 million m^3 of water during 2015–2018. A water table mound was formed beneath the MAR site with a maximum recovery of groundwater levels of more than 10 m. About 40 % of the infiltrated water was captured by pumping wells in the No. 8 well field which contributes directly to the water supply in Beijing.

The effects of the long-term operation of the full-scale MAR were simulated with the coupled multi-scale flow and transport models from 2020 to 2050. The simulation results show that the designed MAR scheme with 9 cascade terraced infiltration ponds in the Chaobai River catchment is very effective in restoring the depleted aquifer storage and maintaining the groundwater abstraction in the No.8 well field. After about 15 years of operation, the cone of the depression and groundwater levels will stabilize as the aquifer system approaches a new equilibrium state. By the year 2050, about 91 % of the total abstraction in the No. 8 well field will come from the infiltrated water. Sustainable groundwater resources development can be achieved in the Chaobai River catchment.

The model results also show that with the increasing groundwater level beneath the infiltration ponds, the infiltration rate of several infiltration ponds will decrease. To maintain a high infiltration rate, groundwater levels beneath the ponds should be kept below the bottom of the ponds. Therefore, groundwater abstractions in the No. 8 well field should be continued with the current capacity. Other environmental problems associated with the rising water table should be investigated which is beyond the scope of this research.

This integrated modelling approach with coupled regional and locale flow and transport processes is an effective tool for designing and assessing MAR schemes. The developed model in this study will be applied to the assess effects of river leakage as a managed aquifer recharge method in the Yongding River in the Beijing Plain. The model approach adopted in this study can also be applied to the design and assessment of MAR projects in the world.

CRediT authorship contribution statement

Sida Liu: Data curation, Formal analysis, Investigation, Methodology, Software, Validation, Visualization, Writing – original draft. **Yangxiao Zhou:** Conceptualization, Project administration, Resources, Supervision, Validation, Writing – review & editing. **Weijia Luo:** Formal analysis, Investigation, Software, Visualization. **Feiran Wang:** Formal analysis, Investigation, Software, Visualization. **Michael E. McClain:** Supervision, Validation, Writing – review & editing. **Xu-sheng Wang:** Supervision, Validation, Writing – review & editing.

Declaration of Competing Interest

The authors declare that they have no known competing financial interests or personal relationships that could have appeared to influence the work reported in this paper.

Data availability

The data that has been used is confidential.

Acknowledgement

Appendix A. Supplementary data

Supplementary data to this article can be found online at https://doi.org/10.1016/j.jhydrol.2022.128392.

References

Abbo, H., Gev, I., 2008. Numerical model as a predictive analysis tool for rehabilitation and conservation of the Israeli coastal aquifer: example of the Shafdan sewage reclamation project. Desalination 226, 47–55.

Aeschbach-Hertig, W., Gleeson, T., 2012. Regional strategies for the accelerating global problem of groundwater depletion. Nat. Geosci. 5, 853–861. https://doi.org/10.1038/ngeo1617.

AQSIQ, SAC, 2017. Standard for Groundwater Quality. CChina.

Aquaveo, 2019. GMS - Groundwater Modeling System 10.4 Tutorials [WWW Document]. URL https://www.aquaveo.com/software/gms-learning-tutorials.

Bahar, T., Oxarango, L., Castebrunet, H., Rossier, Y., Mermillod-Blondin, F., 2021. 3D modelling of solute transport and mixing during managed aquifer recharge with an infiltration basin. J. Contam. Hydrol. 237, 103758 https://doi.org/10.1016/j.jconhyd.2020.103758.

Barber, M.E., Hossain, A., Covert, J.J., Gregory, G.J., 2009. Augmentation of seasonal low stream flows by artificial recharge in the Spokane Valley-Rathdrum Prairie aquifer of Idaho and Washington, USA. Hydrogeol. J. 17, 1459–1470. https://doi.org/10.1007/s10040-009-0467-6.

Beijing Water Authority, 2021. Beijing Water Resources Bulletin (1986-2020) [WWW Document]. Beijing Water Auth. URL http://swj.beijing.gov.cn/zwgk/szygb/ (accessed 11.2.21).

Bouwer, H., 2002. Artificial recharge of groundwater: hydrogeology and engineering. Hydrogeol. J. 10, 121–142. https://doi.org/10.1007/s10040-001-0182-4.

Cao, X., Zhai, Y., Li, M., Pan, C., Zheng, F., Lu, H., Xia, X., Teng, Y., Wang, J., 2022. The suitability assessment of groundwater recharge by leakage of the Yongding River. Hydrogeol. Eng. Geol. 49, 20–29. https://doi.org/10.16030/j.cnki.issn.1000-3665.202107069.

Dillon, P., 2005. Future management of aquifer recharge. Hydrogeol. J. 13, 313–316. https://doi.org/10.1007/s10040-004-0413-6.

Evans, P., Arunakumaren, J., 2012. Groundwater Management in Bribie Island Fo Urban Expansion. Achiev. Groundw. Supply Sustain. Reliab. through Manag. Aquifer Recharg. Proc. 7th Int. Symp. Manag. Aquifer Recharg. 381–388.

Famiglietti, J.S., 2014. The global groundwater crisis. Nat. Clim. Chang. 4, 945–948. https://doi.org/10.1038/nclimate2425.

Gale, I., 2005. Strategies for Managed Aquifer Recharge (MAR) in semi-arid areas. UNESCO.

Ganot, Y., Holtzman, R., Weisbrod, N., Nitzan, I., Katz, Y., Kurtzman, D., 2017. Monitoring and modeling infiltration–recharge dynamics of managed aquifer recharge with desalinated seawater. Hydrol. Earth Syst. Sci. 21, 4479.

Ganot, Y., Holtzman, R., Weisbrod, N., Bernstein, A., Siebner, H., Katz, Y., Kurtzman, D., 2018. Managed aquifer recharge with reverse-osmosis desalinated seawater: modeling the spreading in groundwater using stable water isotopes. Hydrol. Earth Syst. Sci. 22, 6323–6333. https://doi.org/10.5194/hess-22-6323-2018.

Ghayoumian, J., Ghermezcheshme, B., Feiznia, S., Noroozi, A.A., 2005. Integrating GIS and DSS for identification of suitable areas for artificial recharge, case study Meimeh Basin, Isfahan, Iran. Environ. Geol. 47, 493–500. https://doi.org/10.1007/s00254-004-1169-y.

Gleeson, T., VanderSteen, J., Sophocleous, M.A., Taniguchi, M., Alley, W.M., Allen, D.M., Zhou, Y., 2010. Groundwater sustainability strategies. Nat. Geosci. 3, 378–379. https://doi.org/10.1038/ngeo881.

Han, J., 2007. Transient modelling of groundwater flow in Beijing Plain. UNESCO-IHE Institete for Water Education.

Hao, Q., Shao, J., Cui, Y., Xie, Z., 2014. Applicability of artificial recharge of groundwater in the Yongding River alluvial fan in Beijing through numerical simulation. J. Earth Sci. https://doi.org/10.1007/s12583-014-0442-6.

Harbaugh, A.W., 1990. A computer program for calculating subregional water budgets using results from the US Geological Survey modular three-dimensional finite-difference ground-water flow model. US Geological Survey.

Hashemi, H., Berndtsson, R., Persson, M., 2015. Artificial recharge by floodwater spreading estimated by water balances and groundwater modelling in arid Iran. Hydrol. Sci. J.-J. Des. Sci. Hydrol. 60, 336–350. https://doi.org/10.1080/02626667.2014.881485.

Hsieh, H.-H., Lee, C.-H., Ting, C.-S., Chen, J.-W., 2010. Infiltration mechanism simulation of artificial groundwater recharge: a case study at Pingtung Plain, Taiwan. Environ. Earth Sci. 60, 1353–1360. https://doi.org/10.1007/s12665-009-0194-2.

Hu, H., Mao, X., Yang, Q., 2019. Development of a groundwater flow and reactive solute transport model in the Yongding River alluvial fan, China 13, 371–384.

Huang, P.S., Chiu, Y.C., 2018. A simulation-optimization model for seawater intrusion management at Pingtung Coastal Area, Taiwan. Water (Switzerland). https://doi.org/10.3390/w10030251.

IGRAC, 2007. Global MAR Inventory Report.

Izbicki, J.A., Flint, A.L., Stamos, C.L., 2008. Artificial recharge through a thick, heterogeneous unsaturated zone. Ground Water 46, 475–488. https://doi.org/10.1111/j.1745-6584.2007.00406.x.

Jarraya Horriche, F., Benabdallah, S., 2020. Assessing aquifer water level and salinity for a managed artificial recharge site using reclaimed water. Water. https://doi.org/10.3390/w12020341.

Ji, Z., Cui, Y., Zhang, S., Chao, W., Shao, J., 2021. Evaluation of the impact of ecological water supplement on groundwater restoration based on numerical simulation: a case study in the section of yongding river, beijing plain. Water (Switzerland) 13. https://doi.org/10.3390/w13213059.

Jiang, R., Han, D., Song, X., Zheng, F., 2022. Numerical modeling of changes in groundwater storage and nitrate load in the unconfined aquifer near a river receiving reclaimed water. Environ. Sci. Pollut. Res. https://doi.org/10.1007/s11356-022-18597-1.

Karimov, A.K., Smakhtin, V., Mavlonov, A., Borisov, V., Gracheva, I., Miryusupov, F., Akhmedov, A., Anzelm, K., Yakubov, S., Karimov, A.A., 2015. Managed aquifer recharge: potential component of water management in the Syrdarya river basin. J. Hydrol. Eng. 20, 1–12. https://doi.org/10.1061/(asce)he.1943-5584.0001046.

Lacher, L.J., Turner, D.S., Gungle, B., Bushman, B.M., Richter, H.E., 2014. Application of hydrologic tools and monitoring to support managed aquifer recharge decision making in the Upper San Pedro River, Arizona, USA. Water 6, 3495–3527. https://doi.org/10.3390/w6113495.

Lautz, L.K., Siegel, D.I., 2006. Modeling surface and ground water mixing in the Hyporheic zone using MODFLOW and MT3D. Adv. Water Resour. 29, 1618–1633. https://doi.org/10.1016/j.advwatres.2005.12.003.

Liu, S., Zhou, Y., Xie, M., McClain, M.E., Wang, X.-S., 2021b. Comparative assessment of methods for coupling regional and local groundwater flow models: a case study in the Beijing Plain, China. Water. https://doi.org/10.3390/w13162229.

Liu, H.-J., Hsu, N.-S., Lee, T.H., 2009. Simultaneous identification of parameter, initial condition, and boundary condition in groundwater modelling. Hydrol. Process. 23, 2358–2367. https://doi.org/10.1002/hyp.7344.

Liu, S., Zhou, Y., Tang, C., McClain, M., Wang, X.-S., 2021a. Assessment of alternative groundwater flow models for Beijing Plain, China. J. Hydrol. 596, 126065 https://doi.org/10.1016/j.jhydrol.2021.126065.

Ma, X., Yang, Y., Hu, G., Hao, X., Yu, P., Xu, H., Sun, R., Yuan, X., 2020. The impact of eological water supplement of Yongding River on groundwater recharge (in Chinese). Beijing Water 22–27. https://doi.org/10.19671/j.1673.2020.04.005.

Maliva, R.G., Herrmann, R., Coulibaly, K., Guo, W.X., 2015. Advanced aquifer characterization for optimization of managed aquifer recharge. Environ. Earth Sci. 73, 7759–7767. https://doi.org/10.1007/s12665-014-3167-z.

Masetti, M., Pedretti, D., Sorichetta, A., Stevenazzi, S., Bacci, F., 2016. Impact of a storm-water infiltration basin on the recharge dynamics in a highly permeable aquifer. Water Resour. Manag. 30, 149–165. https://doi.org/10.1007/s11269-015-1151-3.

Masetti, M., Pettinato, S., Nghiem, S.V., Paloscia, S., Pedretti, D., Santi, E., 2018. Combining COSMO-SkyMed satellites data and numerical modeling for the dynamic management of artificial recharge basins. J. Hydrol. 567, 41–50. https://doi.org/10.1016/j.jhydrol.2018.09.067.

Mirlas, V., Antonenko, V., Kulagin, V., Kuldeeva, E., 2015. Assessing artificial groundwater recharge on irrigated land using the MODFLOW model. Earth Sci. Res. 4 https://doi.org/10.5539/esr.v4n2p16.

Namjou, P., Pattle, A.D., 2002. Hydrogeological feasibility of disposal of treated effluent in coastal dunes near Auckland, New Zealand, in: Management of Aquifer Recharge for Sustainability: Proceedings of the 4th International Symposium on Artificial Recharge of Groundwater. CRC Press., Adelaide, p. 5. 10.1201/9781003078838.

Nan, T., Shao, J.L., Cui, Y.L., 2016. Column test-based features analysis of clogging in artificial recharge of groundwater in Beijing. J. Groundw. Sci. Eng. 4, 88–95.

Neumann, I., Barker, J., MacDonald, D., Gale, I., 2004. Numerical approaches for approximating technical effectivessness of artificial recharge structures.

Niswonger, R.G., Morway, E.D., Triana, E., Huntington, J.L., 2017. Managed aquifer recharge through off-season irrigation in agricultural regions. Water Resour. Res 53, 6970–6992. https://doi.org/10.1002/2017WR020458.

Olsthoorn, T.N., Mosch, M.J.M., 2002. Fifty years of artificial recharge in the Amsterdam Dune area. Manag. Aquifer Recharg. Sustain. 29–33.

Pliakas, F., Petalas, C., Diamantis, I., Kallioras, A., 2005. Modeling of groundwater artificial recharge by reactivating an old stream bed. Water Resour. Manag. 19, 279–294. https://doi.org/10.1007/s11269-005-3472-0.

Rahman, M., Rusteberg, B., Uddin, M., Lutz, A., Saada, M., Sauter, M., 2013. An integrated study of spatial multicriteria analysis and mathematical modelling for managed aquifer recharge site suitability mapping and site ranking at Northern Gaza coastal aquifer. J. Environ. Manage. 124, 25–39. https://doi.org/10.1016/j.jenvman.2013.03.023.

Ringleb, J., Sallwey, J., Stefan, C., 2016. Assessment of managed aquifer recharge through modeling—A review. Water 8, 579.

Rojas, R., Kahunde, S., Peeters, L., Batelaan, O., Feyen, L., Dassargues, A., 2010. Application of a multimodel approach to account for conceptual model and scenario uncertainties in groundwater modelling. J. Hydrol. 394, 416–435.

Ronayne, M.J., Roudebush, J.A., Stednick, J.D., 2017. Analysis of managed aquifer recharge for retiming streamflow in an alluvial river. J. Hydrol. 544, 373–382. https://doi.org/10.1016/j.jhydrol.2016.11.054.

Russo, T.A., Fisher, A.T., Lockwood, B.S., 2015. Assessment of managed aquifer recharge site suitability using a GIS and modeling. Groundwater 53, 389–400. https://doi.org/10.1111/gwat.12213.

Sashikkumar, M.C., Selvam, S., Kalyanasundaram, V.L., Johnny, J.C., 2017. GIS based groundwater modeling study to assess the effect of artificial recharge: a case study from Kodaganar river basin, Dindigul district, Tamil Nadu. J. Geol. Soc. India 89, 57–64. https://doi.org/10.1007/s12594-017-0558-2.

Soleimani, S., Van Geel, P.J., Isgor, O.B., Mostafa, M.B., 2009. Modeling of biological clogging in unsaturated porous media. J. Contam. Hydrol. 106, 39–50. https://doi.org/10.1016/j.jconhyd.2008.12.007.

Sophocleous, M., 2010. Review: groundwater management practices, challenges, and innovations in the High Plains aquifer, USA—lessons and recommended actions. Hydrogeol. J. 18, 559–575. https://doi.org/10.1007/s10040-009-0540-1.

Teatini, P., Comerlati, A., Carvalho, T., Gutz, A.Z., Affatato, A., Baradello, L., Accaino, F., Nieto, D., Martelli, G., Granati, G., Paiero, G., 2015. Artificial recharge of the phreatic aquifer in the upper Friuli plain, Italy, by a large infiltration basin. Environ. Earth Sci. 73, 2579–2593. https://doi.org/10.1007/s12665-014-3207-8.

UN-water, 2022. The United Nations World Water Development Report 2022: groundwater: making the invisible visible; executive summary. UNESCO.

Vandenbohede, A., Wallis, I., Van Houtte, E., Van Ranst, E., 2013. Hydrogeochemical transport modeling of the infiltration of tertiary treated wastewater in a dune area, Belgium. Hydrogeol. J. 21, 1307–1321. https://doi.org/10.1007/s10040-013-1008-x.

Webber, M., Crow-Miller, B., Rogers, S., 2017. The South-North Water Transfer Project: remaking the geography of China. Reg. Stud. 51, 370–382. https://doi.org/10.1080/00343404.2016.1265647.

Wu, J., Zeng, X., 2013. Review of the uncertainty analysis of groundwater numerical simulation. Chinese Sci. Bull. 58, 3044–3052. https://doi.org/10.1007/s11434-013-5950-8.

Xanke, J., Jourde, H., Liesch, T., Goldscheider, N., 2016. Numerical long-term assessment of managed aquifer recharge from a reservoir into a karst aquifer in Jordan. J. Hydrol. 540, 603–614. https://doi.org/10.1016/j.jhydrol.2016.06.058.

Xu, C., Sun, Y., Shi, B., Wang, X., Li, R., Li, M., Xi, B., Feng, C., 2022. Study on the processes influencing and importance of ecological water replenishment for groundwater resources: a case study in Yongding River. Water. https://doi.org/10.3390/w14050828.

Yao, X., 2014. 北京地下水库建库条件初步分析. 水文水资源 29–32. 10.3969/j.issn.1672-2469.2014.03.011.

Yaraghi, N., Ronkanen, A., Darabi, H., Kløve, B., Torabi Haghighi, A., 2019. Impact of managed aquifer recharge structure on river flow regimes in arid and semi-arid climates. Sci. Total Environ. 675, 429–438. https://doi.org/10.1016/j.scitotenv.2019.04.253.

Zeelie, S., 2002. OMDEL dam and recharge ponds to enhance recharge in the Namib Desert. In: Management of Aquifer Recharge for Sustainability. CRC Press, pp. 387–392.

Zhang, A., Bureau, B.G. and M.R.E. and D., Geology, B.I. of H. and E., 2008. Beijing groundwater (Chinese Edition). China Land Press Pub, Beijing, China.

Zhang, Y., Sun, Y., Wang, X., 2013. Introduction of the Artificial Recharge of Beijing groundwater (In chinese). 城市地质 8, 51–53.

Zheng, C., Wang, P.P., 1999. MT3DMS: a modular three-dimensional multispecies transport model for simulation of advection, dispersion, and chemical reactions of contaminants in groundwater systems; documentation and user's guide. Environmental Laboratory (US).

Zhou, Y.X., Dong, D.W., Liu, J.R., Li, W.P., 2013. Upgrading a regional groundwater level monitoring network for Beijing Plain, China. Geosci. Front. 4, 127–138. https://doi.org/10.1016/j.gsf.2012.03.008.

Zhou, Y., Wang, L., Liu, J., Li, W., Zheng, Y., 2012. Options of sustainable groundwater development in Beijing Plain, China. Phys. Chem. Earth. https://doi.org/10.1016/j.pce.2011.09.001.

Zhou, Y., Olsthoorn, T., Liu, P., 2021. Good Practice for Managed Aquifer Recharge with Infiltration Basins. China Electric Power Press, Beijing.